LAWRENCE
LIVERMORE
NATIONAL
LABORATORY

LLNL-PROC-406224

Crystal Driven Neutron Source: A New Paradigm for Miniature Neutron Sources

V. Tang, J. Morse, G. Meyer, S. Falabella, G. Guethlein, P. Kerr, H. G. Park, B. Rusnak, S. Sampayan, G. Schmid, C. Spadaccini, L. Wang

August 12, 2008

Conference on Accelerator Applications in Research and Industry
Fort Worth, TX, United States
August 11, 2008 through August 15, 2008

Disclaimer

Crystal Driven Neutron Source: A New Paradigm for Miniature Neutron Sources

V. Tang, J. Morse*, G. Meyer, S. Falabella, G. Guethlein, P. Kerr, H. G. Park, B. Rusnak, S. Sampayan, G. Schmid, C. Spadaccini, and L. Wang

Lawrence Livermore National Laboratory, P.O. Box 808, L-229, Livermore, CA 94551
** National Nanomanufacturing Network, University of Massachusetts, Amherst, MA 01027*

Abstract. Neutron interrogation techniques have specific advantages for detection of hidden, shielded, or buried threats over other detection modalities in that neutrons readily penetrate most materials providing backscattered gammas indicative of the elemental composition of the potential threat. Such techniques have broad application to military and homeland security needs. Present neutron sources and interrogation systems are expensive and relatively bulky, thereby making widespread use of this technique impractical. Development of a compact, high intensity crystal driven neutron source is described. The crystal driven neutron source approach has been previously demonstrated using pyroelectric crystals that generate extremely high voltages when thermal cycled [1-4]. Placement of a sharpened needle on the positively polarized surface of the pyroelectric crystal results in sufficient field intensification to field ionize background deuterium molecules in a test chamber, and subsequently accelerate the ions to energies in excess of ~100 keV, sufficient for either D-D or D-T fusion reactions with appropriate target materials. Further increase in ion beam current can be achieved through optimization of crystal thermal ramping, ion source and crystal accelerator configuration. The advantage of such a system is the compact size along with elimination of large, high voltage power supplies. A novel implementation discussed incorporates an independently controlled ion source in order to provide pulsed neutron operation having microsecond pulse width.

Keywords: Neutron source, pyrofusion, crystal, pyroelectric, interrogation
PACS: 29.25.Dz, 77.84.-s, 29.25.Ni, 41.75.Ak

INTRODUCTION

Neutron interrogation techniques have specific advantages for detection of hidden threats over other detection methods in that neutrons readily penetrate most materials, providing backscattered gammas indicative of the elemental composition of the potential threat. Such techniques, especially systems that are portable, have broad application to military and homeland security needs. Multiple interrogation schemes are possible, such as pulsed fast neutron analysis (PFNA) [5], where bursts of neutrons with pulse lengths on the order of 10's of ns or less are sent to a target and used to create backscattered gammas typically from inelastic (n,n') collisions on carbon, nitrogen, and oxygen nuclei. These gammas are then detected using a small time gates ~10-100 ns wide which increases signal to background notably. These data allows the carbon-nitrogen-oxygen ratio of the target to be reconstructed and contraband such as explosives or drugs identified. Other interrogation schemes involving gammas include thermal neutron analysis and associated particle imaging. For all these applications, typically $>\sim 10^6$ n/s are required, with neutron energies greater than the gamma lines of interest for inelastic gamma reactions. Pulsing capabilities are required for PFNA and other interrogation schemes. The D-D and D-T neutron reactions are typically considered.

For any interrogation scheme, a key parameter to detection ability is the signal to background, or R=S/B, which inversely scales with approximately the fourth power of the distance x of the interrogator to target, assuming the neutron source and gamma detector are at the same location. The minimum number of total counts, C, that must be collected for a statistically significant (~1 σ) signal is $C=(R+1)(R+2)/R^2$ [6], which for $R<<1$ implies $C\sim x^8$. Hence, increasing R is very important for applications. In addition to time-gating discussed above, there are two fundamental approaches to increasing R; the first is to create as directional a neutron beam as possible; this typically requires accelerator energies at the MV level and/or exotic reactions. The second approach is to simply bring the source and/or detector closer to the target of interest. Given the above, an ultra-compact, low-cost, and lightweight pulse-able neutron source, or "neutron flare", that could be remoted or even thrown to the target could open up many new interrogation

possibilities or CONOPS. Present commercial sources are simply too large and complex for this operation space. However, the recent development of fusion reactions driven by ~cm scale pyroelectric crystals is promising as the basis for the development of a palm-size neutron source that could satisfy the above requirements. Here, we discuss in detail pyrofusion, experimental and simulation results involving the LLNL Crystal Driven Neutron Source (CDNS) [4], and ongoing work at LLNL on increasing neutron yield and adding pulsing capability to the CDNS.

PYROFUSION

Current pyrofusion systems [1-4] typically combine a small (~3 cm D x 1 cm) cylindrical pyroelectric crystal such as lithium tantalate with a small field emitter tip having typical radius of ~1000 Å mounted on the top face. The crystal is heated or cooled, depending on the polarity of the z-axis, in ~mTorr deuterium gas through the rear face using resistive heaters [1] or peltier heater/coolers [4], to create a large positive voltage, in the ~100 kV range. The electric field at the tip apex is very large, in the >100 MV/cm range, and is able to field ionize deuterium gas in the system, creating at high enough field a purely D+ ion beam [4] that is accelerated onto a deuterated or tritiated target for D-D or D-T fusion reactions. At the end of the first temperature ramp, the system is reset by ramping the temperature in the opposite direction, which results in copious electron current in the 10-100 nA level being emitted. Ideally, if the crystal/emitter can be flipped, both sides of the thermal cycle can be used for ion beam production. A schematic of a typical system is shown in Figure 1. Figure 2 shows the CDNS system which employs a modular crystal assembly with interchangeable field emitter tips, and a peltier heater/cooler system capable of temperature swings from -10 to 110 C. Record neutron data from the CDNS with D-D neutron yields of ~1.9 x 10^5 neutrons per ramp (10 C to 110 C) at the ~10 W level are shown in Figure 3.

A simple model of these pyrofusion systems is described by $dQ/dt=dQ_{pyr}/dt+dQ_{ion}/dt+dQ_{loss}/dt$, where Q is the charge on the crystal surface, Q_{ion} is the charge loss to the ion beam, and Q_{loss} is the parasitic charge loss due to absorbed field emitted electrons from nearby ground planes and the finite resistivity of the crystal. The surface potential is then $V(t)=Q(t)/C$, where $C\sim A(\varepsilon_{cr}/d_{cr}+\varepsilon_0/d)$, d_{cr} is the thickness of the crystal and d the distance to the target or ground plane. Combining this simple potential model with a sophisticated Monte Carlo based model of gas transport near the tip [7], we were able to simulate the current data from [1] as shown in Figure 4 using the experimental temperature as input; at the slow rate of heating used, the crystal temperature is nearly homogenous and hence temperature variation along the z-axis was not considered. The crystal voltage, onset of the ion beam, and beam current can be coarsely controlled by using field emitters with different heights or radii, and by changing the distance from the target to the field emitter [7]. The onset of the ion beam will occur at lower voltage, for example, if the ground plane is closer to the field emitter since that will result in additional field enhancement at the apex. Breakdowns or flashovers over the crystal are not unusual [4].

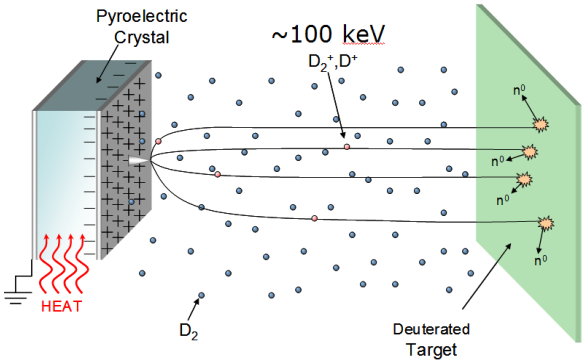

FIGURE 1. Schematic of a typical pyrofusion system.

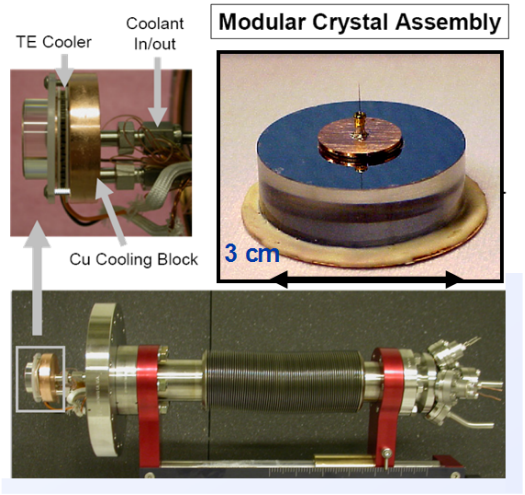

FIGURE 2. Overview of the LLNL CDNS experiment. The modular crystal assembly is mounted on a translatable mount which permits maximum flexibility in the ~8" diameter test chamber.

Currently, pyrofusion systems typically deliver ~10^3 D-D n/s (~2 x 10^5 D-T n/s equivalent) over 100-200 s during each thermal cycle at ~100 kV. In theory, ion currents and neutron intensity could be increased by increasing the voltage through faster thermal cycling and/or by using a taller crystal to decrease the system capacitance. However, in practice, this does not work unless the entire crystal can be heated or cooled very quickly at once—the

large temperature gradients in the crystal caused by heating or cooling only through the rear surface results in field profiles and parasitic currents that negates the effect of larger power input and/or a taller crystal. Some success at increasing the voltage was reported in [3] via the use of two crystals. Lastly, the systems currently considered can not be pulsed easily, considering interrogation schemes that require kHz rep rates and short pulse widths.

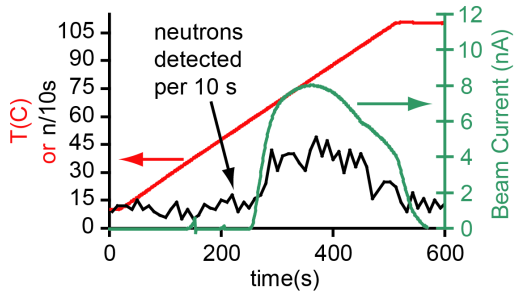

FIGURE 3. Measured beam current (right), detected neutrons per 10 s (left), and rear crystal temperature (left) from the LLNL CDNS. The neutron flat top between t=280–450 s has an average source emission rate of 924±141 n/ s based on a detector efficiency of 0.3%. A total of 1.9±0.3 x 10^5 neutrons was produced by the source from t=0 to t=600 s. Approximately ~40% of the total charge available from the 100 K temperature swing can be attributed to the ion beam and voltage buildup. Adapted from [4].

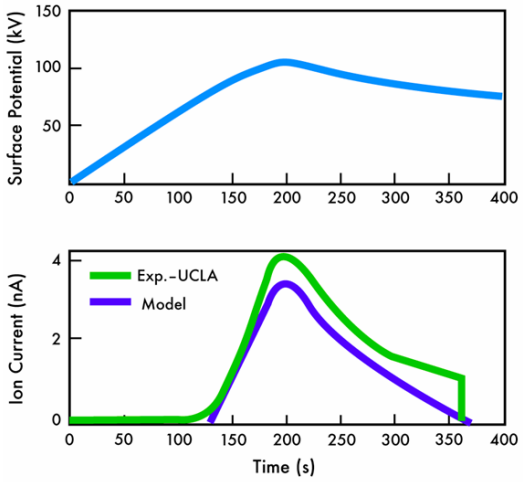

FIGURE 4. Simulation of pyrofusion experiment in [1], using temperature data from Figure 1 of [1]. The predicted current and potential compare well with the experimental result.

From a systems engineering point of view, Table I compares pyrofusion technology with a conventional neutron generator tube modified for battery operation. The key expected advantages of pyrofusion systems over conventional generators are higher neutron yields per kg, significant reduction in system size and weight, and low cost. A potentially large advantage is achieved by the fact that these systems require no electrical power, and can utilize low-level high energy density chemical power sources.

Table I: Comparison of conventional portable neutron generator tube with current pyrofusion source

Modified Activation Technology Corp. portable N550 D-T tube	Single crystal pyrofusion source
▪ ~100 W, ~1-2 hours per charge ▪ Pulse-able, 1 kHz ▪ 28 kg total. 32" long, ~15 liters ▪ <5 x 10^7 D-T n/s ▪ Yield/kg (1 charge): ~10^{10} ▪ Cost: ~$50k	▪ ~100-200 s turn-on per thermal cycle ▪ CW operation ▪ <4.5 kg, palm-size, <500 ml for system ▪ ~2 x 10^5 D-T n/s ▪ Yield/kg(23 kg* fuel, ~10 MJ/kg): ~10^{11} ▪ Cost: ~$1k
* Assume same total weight carried as N550	

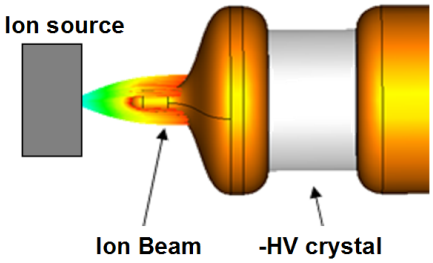

FIGURE 5. Pyrofusion source concept incorporating an independently controlled ion source which is expected to increase neutron intensity significantly and add pulsing capability.

In order to make pyrofusion sources pulse-able and suitable for a larger range of interrogation schemes, we are working on coupling an independently controlled nano-ion source to a pyroelectric crystal operated at negative HV, as schematically shown in Figure 5. By decoupling the ion production from acceleration, this could allow sources that can produce kHz pulses of neutrons. Additionally, the use of a negative HV target focuses the ion beam, in contrast to the divergent beams that are observed for current pyrofusion source using field emitters. We are currently developing and examining various nano-scale ion sources [8], such as nanotube field emission ion sources, gated nanotip arrays, and spark ion sources [9-10] for coupling to the crystal. Using a nanotube field emission ion source, we produced neutrons using a 100 kV test-stand at >10^4 D-D n/s. On the crystal side, we are working on techniques to improve voltage holding and flashover hold-off. Charges losses are inherently greater with a negative HV crystal because of large field emitted currents

from the terminal; field emission based charge losses are not symmetric between positive and negative HV crystals because of the very non-linear dependence of field emission on electric field. One concept [11] we are studying is the use of dielectric fluids for both HV insulation and significantly faster thermal cycling. We achieved voltages of ~300kV using dielectric fluid quenches and have produce electron beams through coupled vacuum tubes during these experiments.

CONCLUSION

Pulse-able, ultra-compact, low cost palm-size pyrofusion neutron sources could enable many new interrogation scenarios in the military and homeland security operation space. We are currently working on incorporating an independently controlled nano-ion source with a negative HV pyroelectric crystal in order to achieve pulsing capabilities for pyrofusion systems and to increase neutron intensity significantly.

ACKNOWLEDGMENTS

This work was supported by the Defense Advanced Research Projects Agency under contract 1026419 and the LLNL Laboratory Directed Research and Development program with the auspices of the U.S. Department of Energy by Lawrence Livermore National Laboratory under contract DE-AC52-07NA27344. Patents Pending.

REFERENCES

1. B. Naranjo, J. Gimzewski, and S. Putterman, Nature, 434, (2005) 1115.
2. J. Geuther and Y. Danon, J. Appl. Phys., 97, (2005) 074109.
3. J. Geuther, Y. Danon, and F. Saglime, Phys. Rev Letts. 96, (2006) 054803-1.
4. V. Tang, G. Meyer, J. Morse et al., Rev. Sci. Inst., 77, (2007) 083501.
5. T. Gozani, Nuc. Inst. Methods A, 353, (1994) 635.
6. Derived from S=C-B and $S=(C+B)^{0.5}$, assuming Poisson statistics.
7. To be published.
8. V. Tang et al., Abs. 363, this conference.
9. S. Falabella et al., Abs. 345, this conference.
10. G. Guethlein et al., Abs. 183, this conference.
11. V. Tang et al., Abs. 360, this conference.